ELSEVIER

Journal of Alloys and Compounds 446–447 (2007) 28–33

Journal of ALLOYS AND COMPOUNDS

www.elsevier.com/locate/jallcom

Structure, chemical bonds and anisotropy in hydrides IMC with $CeNi_3$ and $PuNi_3$ structure

S.A. Lushnikov [a,*], V.N. Verbetsky [a], V.P. Glazkov [b], V.A. Somenkov [b]

[a] *Moscow State University, 119992 Moscow, Russia*
[b] *Russian Research Center, Kurchatov Institute, 123182 Moscow, Russia*

Received 19 September 2006; received in revised form 22 December 2006; accepted 1 January 2007
Available online 13 January 2007

Abstract

Hydrides of $CeNi_3$, $ErNi_3$ and $CeCo_3$ intermetallic compounds have been synthesised under low and high (up to 200 MPa) hydrogen pressure. The structure of the hydrides has been analysed by X-ray and neutron diffraction methods. All hydrides retain the structure of the initial alloys with expanded lattice. The positions and parameters of hydrogen and metallic atoms have been determined and it is established that the anisotropy of the lattice slowly increases for hydrides with high hydrogen concentration. Different anisotropy and expansion of the volume of the lattice $CeNi_3$, $CeCo_3$ and $ErNi_3$ hydrides as have been shown depend of hydrogen concentration, blocks construction of the structure and are determined by the type of chemical bonds between hydrogen and the metallic sublattice, where hydrogen is a donor of the electron for *d*-metal and acceptor of the electron from *f*-metal.

Keywords: Intermetallic compounds (IMC); Hydrides; High pressure of hydrogen; Neutron diffraction

1. Introduction

The behaviour of the structure and volume of the metallic hydrides with different hydrogen concentration is important to understand their type of chemical bond and for the prediction of their capacity for different applications. The most interesting example of hydrogen interaction with intermetallic compounds shows hydrides formed on the basis of RT_3 intermetallics (R-earth-rare metal, T-*d*-metal) with $CeNi_3$ and $PuNi_3$ structural type. Their structure can be considered as a stacking of the well known $MgZn_2$-type and $CaCu_5$-type slabs along the *z*-axis. Has been demonstrated by different methods that some of such intermetallic (R=Ce, La, Pr, Nd) under hydrogenation has large anisotropy of the lattice. Other hydrides with R=Ho, Er have lattice with small anisotropic expansion. This behaviour of intermetallic compounds under hydrogenation may be take place for the reason of the diverse type of the sites, occupied with hydrogen in the lattice or different interaction of hydrogen and metallic atoms.

In several works [1,2,3], have been shown that hydrides of $CeNi_3$ synthesised under low pressure have anomalously large expansion of the lattice along *z*-axis (about 30%), while in the basal plane the lattice has small change of the parameters. Recently Yartys et al. [4] investigated the crystal structure of the $CeNi_3D_{2.8}$ and found an orthorhombic symmetry lowering into the *Pmcn* space group. Deuterium atoms in $CeNi_3D_{2.8}$ are located mostly inside $CeNi_2$ units and fill new site with metallic environment in comparison with the different site position in the hexagonal lattice of $CeNi_3$. In Ref. [5] hydrogenation of $CeNi_3H_{5.6}$ was performed under high hydrogen pressure. X-ray diffraction study of $CeNi_3H_{5.6}$ shows that hydride retained hexagonal unit cell of $CeNi_3$ and has increased cell parameters. In hydrides of $SmRu_{1.2}Co_{1.8}$ and $SmRu_{1.6}Ni_{1.4}$ with $CeNi_3$ structure [6], studied by X-ray diffraction, the anisotropic expansion effect is small. In Ref. [7] it has been shown that in the compounds CeY_2Ni_9 and LaY_2Ni_9 both with the $PuNi_3$ structure, isotropic expansion of the lattice takes place when both RT_2 and RT_5 blocks are filled with hydrogen as case for LaY_2Ni_9, and that anisotropic expansion occurs one RT_2 block is filled as in CeY_2Ni_9. We can expect that with increasing of the hydrogen concentration (under high pressure) will be filled both structural units in RT_3 compounds and isotropic cell volume expansion

* Corresponding author. Tel.: +7 95 939 14 13; fax: +7 95 932 88 46.
E-mail address: lushnikov@hydride.chem.msu.ru (S.A. Lushnikov).

0925-8388/$ – see front matter © 2007 Elsevier B.V. All rights reserved.
doi:10.1016/j.jallcom.2007.01.027

will be appear. The goal of this work is to determine a type of hydrogen sites into structural blocks of the compounds and establish the category of the lattice anisotropy in RT_3 hydrides under high pressure of hydrogen.

2. Experimental

The samples of $CeNi_3$, $ErNi_3$ and $CeCo_3$ alloys prepared by arc-melting pure metals in an inert atmosphere and annealed at 700 °C ($CeNi_3$) and 950 °C ($ErNi_3$ and $CeCo_3$) for 240 h in an evacuated silica tube. Synthesis of the hydrides was carried out on high pressure installation (up to 200 MPa) [8] and under low pressure of hydrogen on the Siverts apparatus. The hydrogen was delivered in small increments to the alloy under moderate pressure (0.1 MPa.) to avoid the amorphous products. Synthesized hydrides were passivated by cooling and holding in liquid nitrogen at 77 K temperature. The amount of absorbed hydrogen was determined by thermal desorption measurements. Deuterium rather than hydrogen has been used to study hydrides in order to reduce the incoherent absorption of neutrons. Neutron diffraction measurements were performed with a DISK diffractometer ($\lambda = 1.66$ Å) at the Russian Research Centre Kurchatov Institute and with High Resolution Fourier Diffractometer (HRFD) at JINR. X-ray diffraction patterns were collected on "ThermoARL" and "Rigaku" diffractometer.

3. Result and discussion

X-ray and neutron examination showed that the $CeNi_3$, $ErNi_3$ and $CeCo_3$ samples were single-phase with lattice parameters corresponding with Refs. [9] (Table 1). From X-ray and neutron diffraction patterns (Figs. 1 and 2) it is shown that $CeNi_3D_{3.3}$, $ErNi_3D_{4.0}$, $CeCo_3D_{4.0}$ deuterides with low concentrations and $CeNi_3D_{5.2}$, $ErNi_3D_{5.0}$, $CeCo_3D_{6.0}$ with high concentration retain the structure of the initial alloys. From the data in Table 1, we can see that hydrides with high concentration have small changes of the volume at each absorbed atom of hydrogen ($\Delta V/H$) and lattice anisotropy c/a, while hydrides with low concentration have large anisotropy and greater changes of $\Delta V/H$. It has been established using neutron diffraction data that in $CeNi_3D_{3.3}$ deuteride with low concentration the deuterium accommodates in $24l_1$, $24l_2$, $12k_1$ sites and with small occupancy in $4f_1$ site (Table 2). Sites $24l_1$ and $12k_1$ have maximum

Table 1
Composition, cell parameters and volume effects for deuterides $CeNi_3$, $ErNi_3$ and $CeCo_3$

Composition	Cell parameters				
	a (Å)	c (Å)	V (Å^3)	$\Delta V/V$ (%)	$\Delta V/H$ (Å^3)[a]
$CeNi_3$	4.964(3)	16.53(1)	353	–	–
$CeNi_3D_{3.3}$	4.934(2)	21.73(3)	458	29.7	5.3
$CeNi_3D_{5.2}$	4.938(3)	22.44(1)	474	34.2	3.9 (1.4[b])
$ErNi_3$	4.943(2)	24.28(2)	514	–	–
$ErNi_3D_{4.0}$	5.271(2)	26.65(2)	641	25.2	3.6
$ErNi_3D_{5.0}$	5.294(3)	26.70(1)	648	26.6	3.0 (0.8[b])
$CeCo_3$	4.961(1)	24.80(3)	529	–	–
$CeCo_3D_{4.0}$	4.936(3)	32.45(2)	684	29.3	4.3
$CeCo_3D_{6.0}$	4.980(1)	32.65(2)	701	32.5	3.2 (0.9[b])

[a] $\Delta V = V(x) - V(0)$, where x is H-to metal atomic rate.
[b] $\Delta V = V(y) - V(x)$, where y is H of high concentration to metal atomic rate and x is H of low concentration to metal rate.

content of the cerium into surrounding (R_2T_2 coordination), while sites $24l_2$ and $4f_1$ with RT_3 coordination have a reduced amount of cerium. Sites $24l_1$ and $4f_1$ are located inside of the RT_2 unit, $24l_2$ inside of the RT_5 unit and site $12k_1$ is located on the border of RT_2 and RT_5 unit. On the neutron patterns of the $CeNi_3D_{5.2}$ with greater deuterium composition is seen a halo presence indicating to amorphous sample (Fig. 1). In the $CeNi_3D_{5.2}$ deuterium filled the same sites as in $CeNi_3D_{3.3}$ but with higher occupancy and also deuterium located in the octahedral $6h_1$ position. In both deuterides deuterium atoms occupies the next sites while nearest neighbours sites are partially occupied. From neutron diffraction data of $ErNi_3D_{4.0}$ and $CeCo_3D_{4.0}$ deuterides with different anisotropy (c/a) and volume effects follows that most of the deuterium is located in $36i_1$ site inside of RT_2 unit (Tables 3 and 4). In $ErNi_3D_{5.0}$ and $CeCo_3D_{6.0}$ deuterides with higher concentration the deuterium occupy partially filled and octahedral sites, which are situated inside of RT_5 unit and on the border of RT_2 and RT_5 unit. From obtained results it is shown that hydrogen atoms occupy first sites inside of RT_2 unit in hydrides with low concentration. In hydrides with a higher

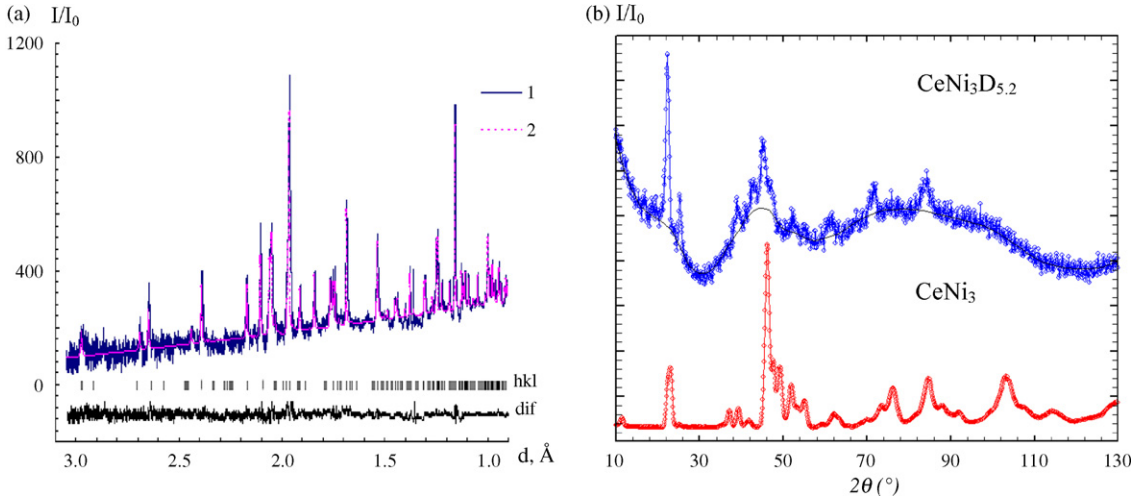

Fig. 1. Neutron diffraction patterns of $CeNi_3D_{3.3}$ (a) obtained by the time of flight method, 1-observed points and 2-calculated intensities, and neutron diffraction patterns of $CeNi_3D_{5.2}$ in comparison with $CeNi_3$ (b).

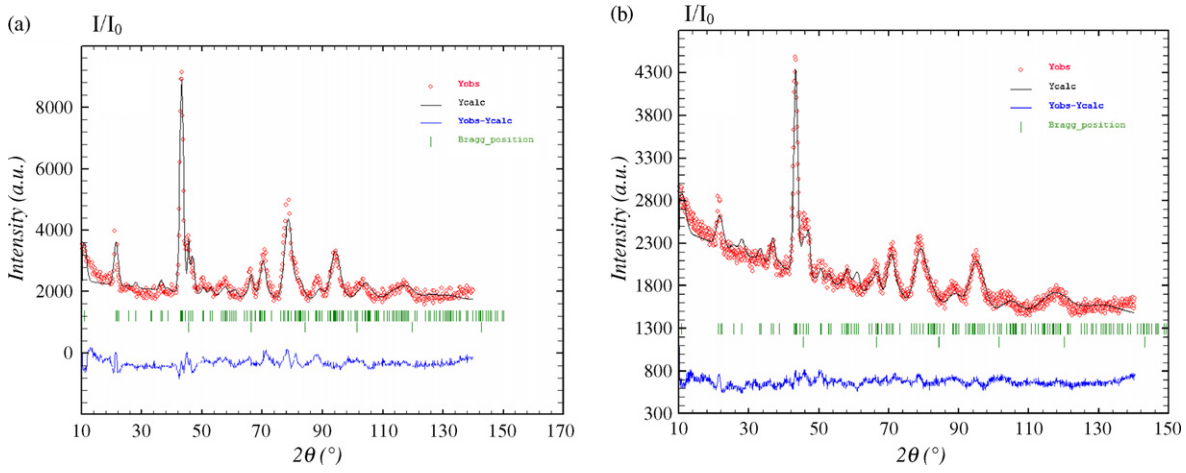

Fig. 2. Neutron diffraction patterns of $ErNi_3D_{4.0}$ (a) and $ErNi_3D_{5.0}$ (b).

Table 2
Structure data for $CeNi_3$ deuterides from neutron powder diffraction

$CeNi_3D_{3.3}$						$CeNi_3D_{5.2}$			
Atom	Site	Number atoms in el. cell	*x*	*y*	*z*	Number atoms in el. cell	*x*	*y*	*z*
Ce1	2*c*	1.0	0.333	0.666	0.25	1.0	0.333	0.666	0.25
Ce2	4*f*	1.0	0.333	0.666	0.061(2)	1.0	0.333	0.666	0.059(3)
Ni1	2*a*	1.0	0	0	0	1.0	0	0	0
Ni2	2*b*	1.0	0	0	0.25	1.0	0	0	0.25
Ni3	2*d*	1.0	0.333	0.666	0.75	1.0	0.333	0.666	0.75
Ni4	12*k*	1.0	0.833(2)	0.666(2)	0.146(1)	1.0	0.833(1)	0.666(1)	0.140(3)
D1	24l_2	6.0(1)	0.802(2)	0.137(1)	0.292(2)	10.3(3)	0.799(2)	0.138(3)	0.289(2)
D2	24l_1	10.1(2)	0.754(1)	0.666(2)	0.443(2)	13.9(2)	0.759(3)	0.669(2)	0.446(2)
D3	4f_1	1.3(1)	0.333	0.666	0.577(1)	0.8(3)	0.333	0.666	0.570(3)
D4	12k_1	3.6(2)	0.401(1)	0.802(1)	0.152(2)	4.9(3)	0.402(2)	0.804(2)	0.144(2)
D5	6*h*	–	–	–	–	2.4(4)	0.166(2)	0.833(2)	0.75
R_p 7.0%, R_w 6.2%, R_b 8.2%, D/IMC 3.5						R_p 12.4%, R_w 8.1%, R_b 14.1%, D/IMC 5.4			

hydrogen concentration the hydrogen atoms are located on sites inside of RT_5 unit. This result proves us that the anisotropy of the lattice does not depend from the hydrogen distribution in structure of the hydrides. It is possible to find out the reason for different anisotropy of the hydrides lattice with analyses of the interatomic distances. Analyses of interatomic distances of the several sites of $CeNi_3D_{3.3}$, $ErNi_3D_{4.0}$ and $CeCo_3D_{4.0}$ deuterides (Tables 5–7) has shown that R-H and T-H distances have equal increase in comparison with initial alloys and deuterium is located into the centre of the site (Fig. 3a). Result of this analysis is in agreement with so called principle of "heredity" of the interatomic distances, presented in Refs. [10,11]. According of this principle for the hydrides with complex lattice all interatomic distances has "heredity" of the distances from the binary hydrides. On other hand for $CeNi_3D_{3.3}$ and $CeCo_3D_{4.0}$ hydrides in most occupied sites 36i_1 and 24l_1 inside of RT_2 block

Table 3
Structure data for $ErNi_3$ deuterides from neutron powder diffraction

$ErNi_3D_{4.0}$						$ErNi_3D_{5.0}$			
Atom	Site	Number atoms in el. cell	*x*	*y*	*z*	Number atoms in el. cell	*x*	*y*	*z*
Er1	3*a*	3.0	0	0	0	3.0	0	0	0
Er2	6*c*	6.0	0	0	0.136(2)	6.0	0	0	0.138(1)
Ni1	3*b*	3.0	0	0	0.5	3.0	0	0	0.5
Ni2	6*c*	6.0	0	0	0.321(2)	6.0	0	0	0.327(2)
Ni3	18*h*	18.0	0.493(1)	−0.493(1)	0.080(3)	18.0	0.503(1)	−0.503(1)	0.081(3)
D1	36i_2	3.6(2)	0.445(3)	0.010(2)	0.003(2)	4.30(3)	0.450(2)	0.006(2)	0.008(2)
D2	18h_3	7.2(2)	0.760(2)	−0.760(3)	0.124(3)	7.60(2)	0.758(2)	−0.758(2)	0.129(2)
D3	36i_1	25.3(2)	0.472(3)	0.008(2)	0.135(3)	28.8(2)	0.469(2)	0.012(2)	0.140(2)
D4	9e_1	–	–	–	–	5.4(1)	0.5	0.5	0
Rp 12.0%, Rw 8.8%, Rb 14.6%, D/IMC 4.0						Rp 11.0%, Rw 8.0%, Rb 12.2%, D/IMC 5.1			

Table 4
Structure data for $CeCo_3$ deuterides from neutron powder diffraction

$CeCo_3D_{4.0}$						$CeCo_3D_{6.0}$			
Atom	Site	Number atoms in el. cell	*x*	*y*	*z*	Number atoms in el. cell	*x*	*y*	*z*
Ce1	3*a*	3.0	0	0	0	3.0	0	0	0
Ce2	6*c*	6.0	0	0	0.127(2)	6.0	0	0	0.125(1)
Co1	3*b*	3.0	0	0	0.5	3.0	0	0	0.5
Co2	6*c*	6.0	0	0	0.321(2)	6.0	0	0	0.327(2)
Co3	18*h*	18.0	0.502(1)	−0.502(1)	0.063(3)	18.0	0.504(1)	−0.504(1)	0.064(4)
D1	$18h_2$	8.50(3)	0.850(2)	−0.850(2)	0.068(3)	10.80(3)	0.843(2)	−0.843(2)	0.070(2)
D2	$36i_1$	27.80(3)	0.461(2)	0.009(4)	0.127(3)	21.20(2)	0.462(3)	0.010(1)	0.129(3)
D3	$36i_2$	–	–	–	–	14.80(2)	0.450(2)	0.012(3)	−0.003(2)
D4	$9e_1$	–	–	–	–	5.90(2)	0.5	0.5	0.0
Rp 9.2%, Rw 9.0%, Rb 15.1%, D/IMC 4.0						Rp 11.6%, Rw 10.7%, Rb 12.4%, D/IMC 5.9			

Table 5
Interatomic distances in $CeCo_3$ compound and deuterides, *d* (Å)

Type of site and block	$CeCo_3$	$CeCo_3D_{4.0}$	$CeCo_3D_{6.0}$
$18h_2$	Ce_1-Ce_2 3.05	Ce_1-Ce_2 3.82 Ce_1-D 2.75	Ce_1-Ce_2 4.15 Ce_1-D 2.66
RT_2 and RT_5	Ce_1-Co_3 2.81	Ce_1-Co_3 3.22 Ce_2-D 2.51	Ce_1-Co_3 3.25 Ce_2-D 2.30
	Ce_2-Co_3 2.71	Ce_2-Co_3 3.12 Co_3-D 1.51	Ce_2-Co_3 3.23 Co_3-D 1.48
	Co_3-Co_3 2.61	Co_3-Co_3 2.43	Co_3-Co_3 2.47
$36i_1$	Ce_2-Ce_2 2.55	Ce_2-Ce_2 3.82 Ce_2-D 2.55	Ce_2-Ce_2 3.87 Ce_2-D 2.68
RT_2	Ce_2-Co_3 2.51	Ce_2-Co_3 4.81 Ce_2-D 2.51	Ce_2-Co_3 4.85 Ce_2-D 2.30
	Ce_2-Co_3 2.50	Ce_2-Co_3 3.21 Co_3-D 2.53	Ce_2-Co_3 3.23 Co_3-D 2.13
	Ce_2-Co_1 2.51	Ce_2-Co_1 3.12 Co_1-D 1.66	Ce_2-Co_1 3.15 Co_1-D 1.89
	Co_3-Co_1 2.53	Co_3-Co_1 3.63	Co_3-Co_1 3.66
$36i_2$	Ce_1-Co_2 2.86	Ce_1-Co_2 2.88	Ce_1-Co_2 2.88 Ce_1-D 2.21
RT_5	Ce_1-Co_3 3.22	Ce_1-Co_3 3.21	Ce_1-Co_3 3.25 Co_2-D 1.52
	Co_2-Co_3 2.53	Co_2-Co_3 2.83	Co_2-Co_3 2.73 Co_3-D 2.21
	Co_2-Co_2 2.86	Co_2-Co_2 2.96	Co_2-Co_2 2.89
$9e_1$	Ce_1-Co_2 2.86	Ce_1-Co_2 2.88	Ce_1-Co_2 2.88 Ce_1-D 2.49
RT_5	Ce_1-Co_2 2.86	Ce_1-Co_2 2.88	Ce_1-Co_2 2.88 Co_2-D 1.45
	Ce_1-Co_3 3.22	Ce_1-Co_3 3.21	Ce_1-Co_3 3.25 Co_3-D 2.09
	Co_2-Co_3 2.49	Co_2-Co_3 2.19	Co_2-Co_3 2.35
Interatomic distances, *d* (Å) [10] for Ce-H 2.42 (binary hydride) and Co-H 1.86			

Table 6
Interatomic distances in $ErNi_3$ compound and deuterides, *d* (Å)

Type of site and block	$ErNi_3$	$ErNi_3D_{4.0}$	$ErNi_3D_{5.0}$
$36i_2$	Er_1-Ni_2 2.95	Er_1-Ni_2 3.01 Er_1-D 2.25	Er_1-Ni_2 3.06 Er_1-D 2.38
RT_5	Er_1-Ni_3 2.83	Er_1-Ni_3 2.91 Ni_2-D 1.51	Er_1-Ni_3 3.42 Ni_2-D 1.53
	Ni_2-Ni_2 2.51	Ni_2-Ni_2 2.51 Ni_3-D 1.43	Ni_2-Ni_2 3.08 Ni_3-D 1.77
	Ni_1-Ni_2 2.21	Ni_1-Ni_2 2.41	Ni_2-Ni_3 2.80
$18h_3$	Er_2-Er_2 2.85	Er_2-Er_2 3.05 Er_2-D 2.23	Er_2-Er_2 3.41 Er_2-D 2.55
RT_2	Er_2-Ni_3 2.51	Er_2-Ni_3 2.91 Ni_3-D 1.80	Er_2-Ni_3 3.05 Ni_3-D 1.87
	Ni_3-Ni_3 2.41	Ni_3-Ni_3 2.51	Ni_3-Ni_3 2.60
$36i_1$	Er_2-Er_2 2.99	Er_2-Er_2 3.14 Er_2-D 2.43	Er_2-Er_2 3.42 Er_2-D 2.45
RT_2	Er_2-Ni_1 2.89	Er_2-Ni_1 2.92 Ni_3-D 1.48	Er_2-Ni_1 3.15 Ni_3-D 1.59
	Er_2-Ni_3 2.95	Er_2-Ni_3 3.06 Ni_1-D 1.52	Er_2-Ni_3 3.10 Ni_1-D 1.73
	Ni_1-Ni_3 2.32	Ni_1-Ni_3 2.47	Ni_1-Ni_3 2.77
$9e_1$	Er_1-Ni_2 2.86	Er_1-Ni_2 3.06	Er_1-Ni_2 3.04 Er_1-D 2.64
RT_5	Er_1-Ni_2 2.86	Er_1-Ni_2 3.06	Er_1-Ni_2 3.04 Ni_2-D 1.54
	Er_1-Ni_3 3.15	Er_1-Ni_3 3.39	Er_1-Ni_3 3.42 Ni_3-D 2.16
	Ni_3-Ni_2 2.21	Ni_3-Ni_2 2.40	Ni_3-Ni_2 2.50
Interatomic distances, *d* (Å) [10] for Er-H 2.22 (binary hydride) Ni-H 1.82			

Table 7
Interatomic distances in $CeNi_3$ compound and deuterides, d (Å)

Type of site and block	$CeNi_3$	$CeNi_3D_{3,3}$	$CeNi_3D_{5,2}$
$24l_2$	Ce_1-Ni_3 2.86	Ce_1-Ni_3 2.85 Ce_1-D 2.78	Ce_1-Ni_3 2.85 Ce_1-D 2.79
RT_5	Ce_1-Ni_4 3.20	Ce_1-Ni_4 3.38 Ni_2-D 1.71	Ce_1-Ni_4 3.49 Ni_2-D 1.73
	Ce_1-Ni_2 2.86	Ce_1-Ni_2 2.85 Ni_3-D 1.70	Ce_1-Ni_2 2.85 Ni_3-D 1.71
	Ni_2-Ni_3 2.86	Ni_2-Ni_3 2.85 Ni_4-D 1.40	Ni_2-Ni_3 2.85 Ni_4-D 1.51
	Ni_2-Ni_4 2.49	Ni_2-Ni_4 2.71	Ni_2-Ni_4 2.85
	Ni_3-Ni_4 2.49	Ni_3-Ni_4 2.71	Ni_3-Ni_4 2.85
	Ce_2-Ce_2 3.18	Ce_2-Ce_2 3.92 Ce_2-D 2.50	Ce_2-Ce_2 3.89 Ce_2-D 2.90
$24l_1$	Ce_2-Ni_1 2.94	Ce_2-Ni_1 3.15 Ce_2-D 2.50	Ce_2-Ni_1 3.14 Ce_2-D 2.10
RT_2	Ce_2-Ni_4 3.14	Ce_2-Ni_4 4.70 Ni_1-D 1.92	Ce_2-Ni_4 4.69 Ni_1-D 1.96
	Ce_2-Ni_4 2.85	Ce_2-Ni_4 3.04 Ni_4-D 1.88	Ce_2-Ni_4 3.07 Ni_4-D 1.90
	Ni_1-Ni_4 2.54	Ni_1-Ni_4 3.44	Ni_1-Ni_4 3.45
	Ce_1-Ce_2 3.44	Ce_1-Ce_2 4.09 Ce_1-D 2.25	Ce_1-Ce_2 4.27 Ce_1-D 2.45
$12k_1$	Ce_1-Ni_4 3.21	Ce_1-Ni_4 3.38 Ce_2-D 2.20	Ce_1-Ni_4 3.49 Ce_2-D 2.20
RT_2 and RT_5	Ce_2-Ni_4 2.86	Ce_2-Ni_4 3.04 Ni_4-D 1.87	Ce_2-Ni_4 3.07 Ni_4-D 1.89
	Ni_4-Ni_4 2.48	Ni_4-Ni_4 2.47	Ni_4-Ni_4 2.44
$4f_1$	Ce_2-Ni_4 3.14	Ce_2-Ni_4 4.70 Ce_2-D 3.00	Ce_2-Ni_4 4.71 Ce_2-D 3.04
RT_2	Ni_4-Ni_4 2.48	Ni_4-Ni_4 2.47 Ni_4-D 2.08	Ni_4-Ni_4 2.48 Ni_4-D 2.05
$6h_1$	Ce_1-Ni_2 2.86	Ce_1-Ni_2 2.85	Ce_1-Ni_2 2.86 Ce_1-D 2.47
RT_5	Ce_1-Ni_3 2.86	Ce_1-Ni_3 2.85	Ce_1-Ni_3 2.86 Ni_2-D 1.43
	Ce_1-Ni_4 3.20	Ce_1-Ni_4 3.38	Ce_1-Ni_4 3.49 Ni_3-D 1.43
	Ni_2-Ni_4 2.49	Ni_2-Ni_4 2.85	Ni_2-Ni_4 2.85 Ni_4-D 2.48
	Ni_3-Ni_4 2.49	Ni_3-Ni_4 2.85	Ni_3-Ni_4 2.85

Interatomic distances, d (Å) [10] for Ce-H 2.42 (binary hydride) Ni-H 1.82

we can see increases of the T-H distance (in case of $CeCo_3D_{4.0}$ this increases is substantial, Tables 5–7) in comparison with distances of the binary hydrides (NiH_x, CoH_x). At the same time as the R-H distances stay approximately as in the binary hydride (CeH_2, Tables 5–7; Fig. 3b). Increasing of the T-H distance happens because of the large and negatively charged hydrogen atom (hydrogen receive electron from R-atom) "pushing out" the T-atom. Difference in R-H and T-H interatomic distances in comparison with the distances in binary hydrides takes place as a result of differently charged hydrogen atoms. This is the reason the different volume effects and anisotropy of the lattice with increasing hydrogen concentration in the RT_3 hydrides. Such behaviour of the hydrogen must be more remarkably for intermetallic compounds containing earth-rare atoms (La, Ce, Pr, Nd), which easy donate electrons to *sp*-zone and having typical valence state R^{+4+3} (Ce, Pr) [12]. For compounds with earth-rare atoms as Dy, Ho, Er having usual valence state R^{+3+2} this behaviour display weakly. In case of *d*-metals the increasing of volume effects of the lattice must display stronger in T-ions with filled *d*-zone. So different volume effects and anisotropy of the lattice can be explained on the basis of the different character of the chemical bond of hydrogen with diverse metals into intermetallic, where hydrogen is acceptor electrons from R-metal and donor for *d*-metal. This explanation was mentioned first in Ref. [13] and was based on expected data about hydrogen distribution in the intermetallic matrix. Obtained experimental results in this work and data from references confirm this suggestion and show that lattice distortion of RT_3 hydrides depends from hydrogen concentration, his distribution inside blocks and type of chemical bond of the hydrogen with R and T-metals.

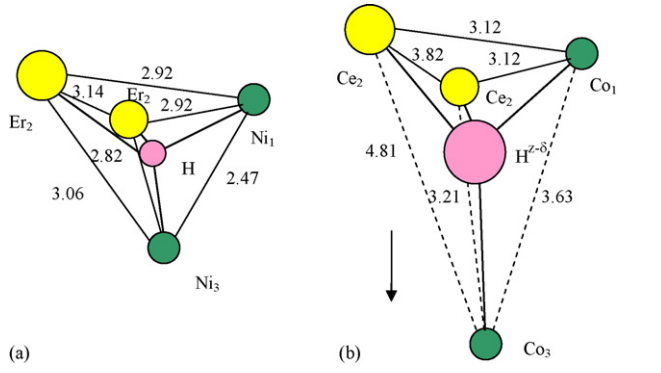

Fig. 3. Situation of the hydrogen atom inside of the site $36i_1$ in the lattice with small anisotropy (a) for $ErNi_3D_{4.0}$ and with large anisotropy of the lattice (b) for $CeCo_3D_{4.0}$.

4. Conclusions

Neutron diffraction data obtained for $CeNi_3$, $ErNi_3$ and $CeCo_3$ hydrides with different concentration have demonstrated that hydrides retain the structure of the initial alloys with expanded lattice and changed parameters of metallic atoms. In hydrides with low concentration hydrogen occupy sites inside RT_2 block, then with increasing concentration, sites on the border RT_2 and RT_5 blocks, and at last inside RT_5 block. Hydrogen atoms interact inside the hydrogen sublattice in the metal matrix and this is a reason for the incompletely occupancies of the sites in hydrides with low concentration. Hydrogenation of RT_3 intermetallic compounds is accompanied with a large anisotropic expansion of the lattice of the Ce-containing hydrides with low

concentration and small anisotropy of the Er-containing hydride. In hydrides with higher hydrogen concentration the anisotropic expansion effect is relatively small. Such behaviour of hydrides is due to the different type of the chemical bond between hydrogen and metals: particularly ionic bond for R-metals and metallic bond for *d*-metals.

Acknowledgments

This work was supported by Russian Foundation for Basic Research, grants No. 03-03-33023 and No. 03-02-17387.

References

[1] R.H. Van Essen, K.H.J. Bushow, J. Less-Common Met. 70 (1980) 189–198.
[2] V.V. Burnasheva, B.P. Tarasov, K.N. Semenenko, J. Neorg. Chem. 27 (12) (1982) 3039–3042.
[3] V.A. Yartys, Inorg. Mater. 18 (4) (1982) 401–408 (in Russian).
[4] V.A. Yartys, O. Isnard, A.V. Riabov, L.G. Akselrud, J. Alloys Compd. 356–357 (2003) 109–113.
[5] V.N. Verbetsky, S.N. Klyamkin, A.Yu. Kovriga, A.P. Bespalov, Int. J. Hydrogen Energy 11–12 (1996) 997–1000.
[6] A.L. Shilov, E.I. Yaropolova, M.E. Kost, Inorg. Mater. 252 (6) (1980) 1397–1400 (in Russian).
[7] M. Latroche, V. Paul-Boncour, A. Percheron-Guegan, J. Solid State Chem. 177 (2004) 2542–2549.
[8] V.N. Verbetsky, S.N. Klyamkin, J. Alloys Compd. 194 (1993) 41–45.
[9] K. Teylor, Intermetallic Compounds of Earth-Rare Metals, Mir, Moscow, 1974.
[10] V.A. Somenkov, S.Sh. Shilshtein, J. Phys. Met. 86 (3) (1998) 114–122 (in Russian).
[11] V.A. Somenkov, A.V. Irodova, J. Les-Common Met. 101 (1984) 481–484.
[12] V.A. Shaburov, J. Phys. Solid State 4 (8) (1998) 1393–1396 (in Russian).
[13] K.N. Semenenko, V.V. Burnasheva, Vestn. MSU Chem. 18 (5) (1977) 618–632 (in Russian).